

# Charge-transfer reactions in $\text{Kr}_N(\text{NF}_3)_m$ clusters excited with synchrotron radiation

L. Museur<sup>1,a</sup>, A.V. Kanaev<sup>1,b</sup>, M.C. Castex<sup>1</sup>, L. Moussavizadeh<sup>2</sup>, R. von Pietrowski<sup>3</sup>, and T. Möller<sup>3</sup>

<sup>1</sup> Laboratoire de physique des lasers CNRS, 93430 Villetaneuse, France

<sup>2</sup> II. Institut für Experimentalphysik, Uni. Hamburg, Germany

<sup>3</sup> Hamburger Synchrotronstrahlungslabor HASYLAB am Deutschen Elektronen-Synchrotron DESY, Notkestraße 85 - 22603 Hamburg, Germany

Received: 26 January 1999 / Received in final form: 4 March 1999

**Abstract.** Charge-transfer reactions are observed in a photoluminescence study of  $\text{NF}_3$ -doped free krypton clusters. They show up in emissions from  $\text{Kr}^+\text{F}^-$  free excimers ejected from the clusters, and from excited  $\text{Kr}_2^+\text{F}^-$  and  $\text{Kr}_2^+(\text{NF}_3)_m^-$  ( $m \geq 1$ ) solvated in the clusters. The results show that reaction dynamics in clusters differs considerably from that in the gas and solid phases.

**PACS.** 36.40.-c Atomic and molecular clusters – 82.50.-m Photochemistry and radiation chemistry – 78.55.-m Photoluminescence

## 1 Introduction

Charge-transfer reactions between excited rare-gas atoms ( $\text{Rg}^*$ ) and halogen-containing molecules ( $\text{MX}$ ), so-called “harpoon” reactions, are well-characterized in the gas (see [1–3] and references therein) and solid phases [4–8]. They constitute an important class of chemical reactions which play a key role in excimer laser kinetics [9]. These reactions can be activated either by one vacuum ultraviolet (VUV) photon excitation or by two UV photons excitation in a sequential or coherent process. Whereas the reaction in the gas phase leads to the formation of  $\text{Rg}^+\text{X}^-$  or  $\text{Rg}_2^+\text{X}^-$  excimer depending on the pressure, in homogenous solid matrices, due to the presence of surrounding Rg atoms, only the triatomic excimers  $\text{Rg}_2^+\text{X}^-$  are observed. Although rare-gas clusters may serve as a model system for the characterization of different solid-state properties and gas-to-solid transitions, only recently they appear as attractive species for the study of charge-transfer reactions [10, 11]. It has been shown that for small cluster size ( $N < 10$ ), two-photon excitation [10] of the  $\text{XeCl}_2$  van der Waals complex or one VUV photon excitation of the  $(\text{Xe}^+-\text{Cl}_2^-)$  charge-transfer state [11] result in the formation of  $\text{XeCl}^*(\text{B}, \text{C})$  exciplex. In our first spectroscopical study [12] devoted to  $\text{Rg}_N(\text{NF}_3)$  cluster ( $\text{Rg} = \text{Ar}, \text{Kr}, \text{Xe}$ ), excited into the first absorption band of Rg-cluster, we have followed peculiarities of charge-transfer reactions in a large size domain  $4 \leq N \leq 500$ . The main feature of these reactions is the change of the

reactivity with the size. In small clusters the ejection of excited reaction products ( $\text{Rg}^+\text{F}^-$  excimer) is important due to an excess of kinetic energy and/or the sign of the cluster electron affinity. In the larger clusters creation of excited  $\text{Rg}_2^+\text{F}^-$  centers is observed to be the main reaction yield.

In this letter, we demonstrate the specificity of charge-transfer reactions in  $\text{Kr}_N(\text{NF}_3)_m$  clusters at high degree of doping ( $m \geq 1$ ). It is shown that these reactions are inherently sensitive to the local environment, which, in cluster phase, can be continuously modified by the size effect and the degree of doping. These specific conditions favor different reactions with specific production yield. In particular, we observe the competition between the formation of  $\text{Kr}^+\text{F}^-$ ,  $\text{Kr}_2^+\text{F}^-$  and  $\text{Kr}_2^+(\text{NF}_3)_{m \geq 1}^-$  excimers.

## 2 Experiment

The experiments were performed at the set-up CLULU at HASYLAB (DESY) [13]. In short,  $\text{Kr}_N$  ( $N \sim 2\text{--}400$ ) clusters are prepared in a free expansion of neat krypton gas at a stagnation pressure up to 5 bar and room temperature (300 K) through a conical nozzle ( $d = 100 \mu\text{m}$ ,  $\theta/2 = 15^\circ$ ). The crossed-beam of  $\text{NF}_3$  molecules, prepared in an expansion through a  $300 \mu\text{m}$  nozzle, intersects the cluster beam 15 mm downstream.  $\text{Kr}_N(\text{NF}_3)_m$  clusters are prepared by the pick-up technique. Background pressure  $\leq 10^{-4}$  mbar was maintained during the experiment runtime by a continuous pumping of the interaction volume. Tunable monochromatized synchrotron radiation in the VUV range ( $\Delta\lambda_{\text{exc}} = 0.25 \text{ nm}$ ) is focused on the cluster beam. The UV-visible fluorescence is analyzed by a

<sup>a</sup> e-mail: museur@lpl.univ-paris13.fr

<sup>b</sup> Present address: LIMHP CNRS, Université Paris-Nord, 93430 Villetaneuse, France.

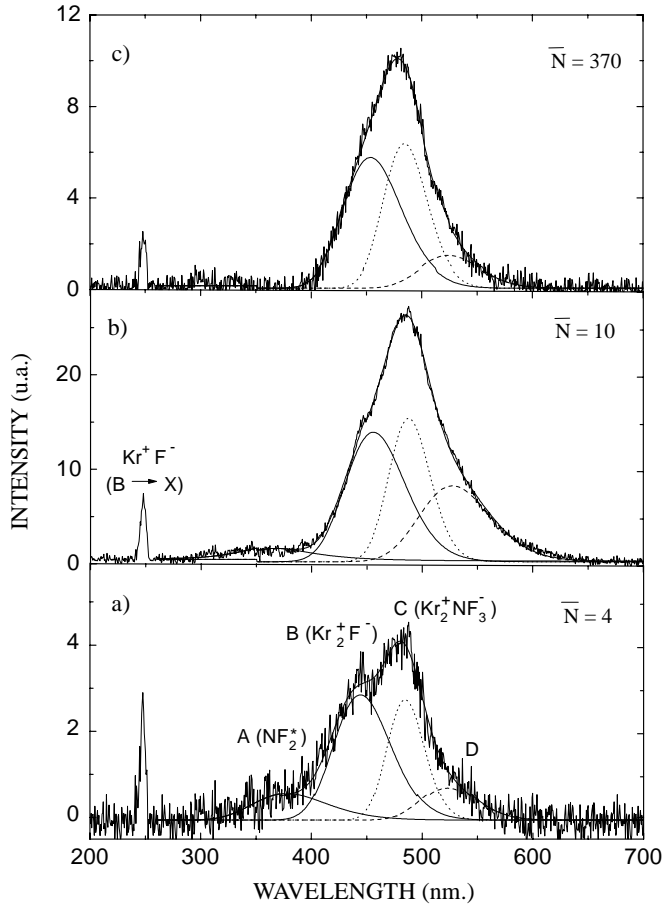


**Fig. 1.** Fluorescence spectra for different sizes of krypton clusters doped at the same flow of  $\text{NF}_3$  ( $p_{\text{NF}_3} = 10$  mbar) and excited with 10 eV photons.

monochromator ( $f = 275$  mm, 150 l/mm, 300  $\mu\text{m}$  slits) equipped with an intensified CCD array detector (Princeton Instruments). Spectra were collected during 300 s. Simultaneously, the total VUV fluorescence was detected by a channelplate detector coated with CsI behind a LiF window. For a given stagnation pressure and temperature of the gas before expansion, the mean cluster size  $\bar{N}$  has been calculated using the experimental calibration curve [13].

### 3 Results

Fluorescence spectra, obtained for different cluster sizes, with 10.0 eV excitation (which correspond to a strong absorption band of krypton clusters), and at fixed  $\text{NF}_3$  cross-beam flow (stagnation pressure  $p_{\text{NF}_3} = 10$  mbar), are shown in Figure 1. Except for the fluorescence at  $\sim 5$  eV which has been assigned to  $\text{Kr}^+\text{F}^-$  ( $\text{B} \rightarrow \text{X}$ ) free excimers ejected from the clusters, we observe a structured broad emission where, at least, three bands are easily visible (see Fig. 1a). This is an unexpected result since in gas or solid phases only one broad Gaussian band, corresponding to  $\text{Kr}_2^+\text{F}^-$  fluorescence, is observed in the visible range of the spectrum [6,9]. We have fitted the broad continua by a sum of Gaussian curves (on the energy scale).

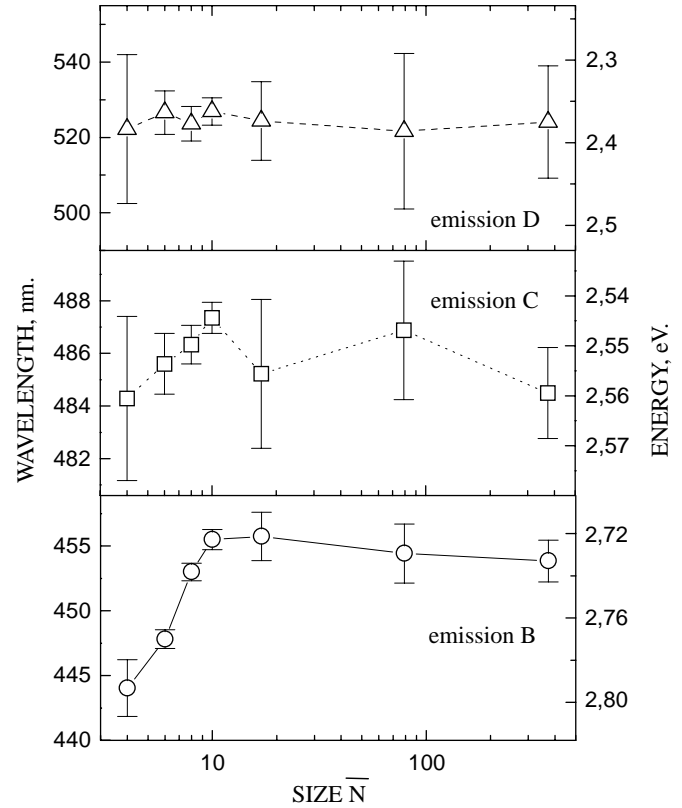


**Fig. 2.** Emission maxima of B, C and D bands as a function of the mean cluster size  $\bar{N}$ .

One should note that the same minimum number of Gaussian continua, which guarantees a satisfactory fit for all the cluster sizes, has been used in each case. Depending on cluster mean size  $\bar{N}$  up to 4 bands, labeled by letters A ( $\sim 3.45$  eV), B ( $\sim 2.73$  eV), C ( $\sim 2.55$  eV) and D ( $\sim 2.40$  eV), have been resolved in the spectra. Moreover, in order to avoid any ambiguity of the fit, we have fixed the width of the  $\text{Kr}_2^+\text{F}^-$  emission (band B) to its value in solid krypton, namely  $\Delta\nu_{\text{B}} = 0.38$  eV [6]. With these conditions, the fit gave reproducible and consistent results concerning spectral positions and widths of the Gaussian continua. In particular, the widths of the bands C and D ( $\Delta\nu_{\text{C}} = 0.22 \pm 10\%$  eV and  $\Delta\nu_{\text{D}} = 0.27 \pm 10\%$  eV) do not vary with the cluster size. The weak emission band A shifts progressively towards the blue and disappears in clusters larger than  $\bar{N} = 10$ . Evolution of the energy positions of the B, C and D bands as a function of  $\bar{N}$  is shown in Figure 2. In contrast to the band B, which undergoes a strong red shift with growing cluster size, the spectral positions of the bands C and D are almost constant.

To understand the origin of these bands, we have examined the effect of doping a cluster by more than one  $\text{NF}_3$  molecule. Change in the cluster doping has been achieved by increasing the  $\text{NF}_3$  stagnation pressure at a constant  $\text{Kr}_N$  cluster flow ( $\bar{N} = 370$ ). Some typical spectra are presented in Figures 1c and 3. Using the same approach, we have fitted the broad asymmetric emission with a sum of Gaussian curves. At a low degree of cluster

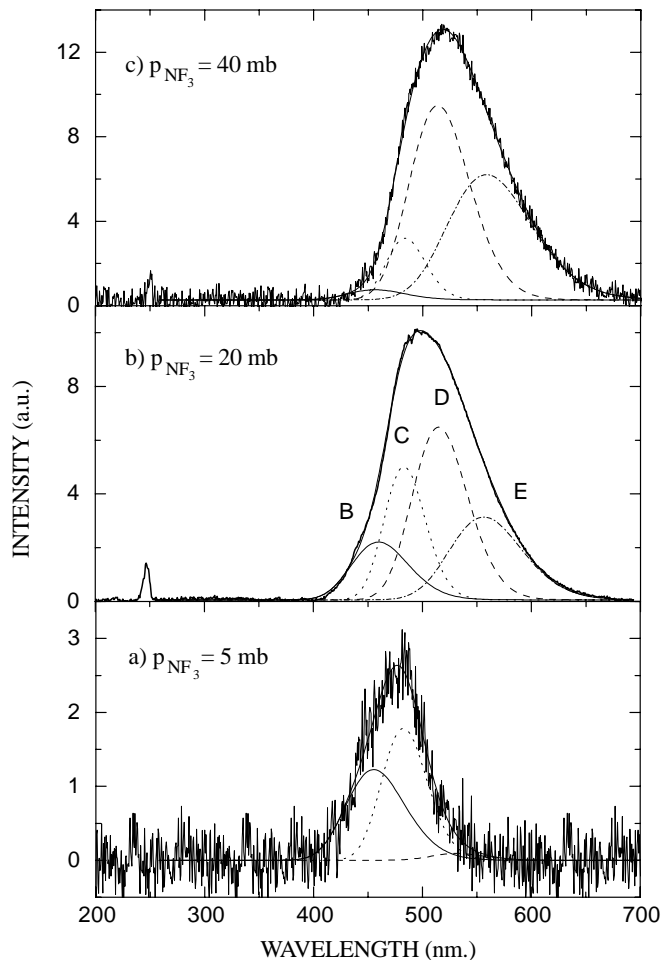


**Fig. 3.** Fluorescence spectra of  $\text{Kr}_N(\text{NF}_3)_m$  (mean size  $\bar{N} = 370$ ) for different static pressures of  $\text{NF}_3$ .

doping ( $p_{\text{NF}_3} = 5$  mbar, Fig. 3a) the fluorescence band has been successfully decomposed into the two Gaussian bands B and C previously used. An introduction of the fourth band D is necessary to fit the spectra observed for cross beam pressure  $p_{\text{NF}_3} = 10$  mbar (Fig. 1c). Moreover, to fit correctly the spectra obtained with the two highest  $\text{NF}_3$  stagnation pressures ( $p_{\text{NF}_3} = 20$  or 40 mbar), we have been obliged to introduce another emission band, E (2.21 eV), red shifted with respect to the band D. This band E is absolutely not detected in the spectra obtained at lower  $\text{NF}_3$  stagnation pressure ( $p_{\text{NF}_3} < 20$  mbar). Finally, this global fit procedure, in which we introduce five emissions bands, allows us to reproduce all observed modifications of the emission spectra either when varying the mean size of the krypton cluster or when varying the number of  $\text{NF}_3$  molecules deposited on it.

In Figure 3 we can observe that the intensity of the band D increases with the  $\text{NF}_3$  gas flow. At the same time, the intensity of the bands B and C continuously decreases. The evolution of the fluorescence intensities as a function of  $\text{NF}_3$  stagnation pressure is shown in Figure 4. Assignments of the emission bands and peculiarities of the

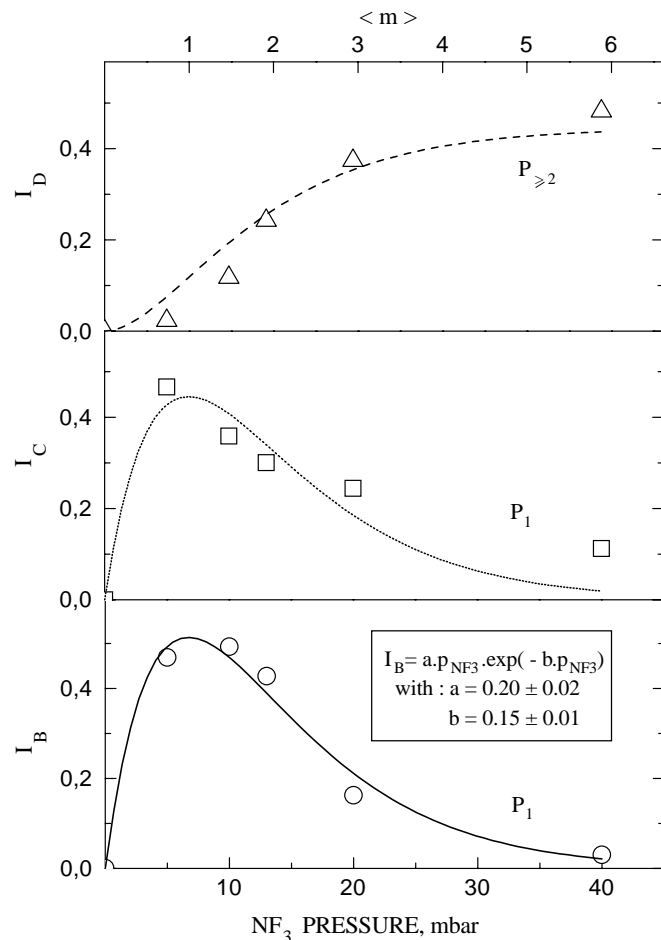


**Fig. 4.** Relative intensity of emissions bands B, C and D as a function of the  $\text{NF}_3$  static pressure.

reaction as a function of the cluster size and  $\text{NF}_3$  pressure are discussed below.

## 4 Discussion

We have tentatively ascribed the band A to the  $\text{NF}_2^*$  excited radical. Fluorescence around 300 nm has been observed under e-beam excitation of  $\text{NF}_3$  gas beam [14]. Under our experimental conditions the  $\text{NF}_2^*$  radicals are presumably produced by a direct photodissociation of  $\text{NF}_3$ , or after an energy transfer from  $\text{Kr}_N^*$ . More precise analysis would be possible if information about  $\text{NF}_2^*$  fluorescence spectroscopy could be found in the literature.

In contrast to the fixed spectral position and shape of the UV emission band at 5 eV assigned to the  $\text{KrF}^*$  excimers ejected from the cluster, the band B displays a cluster size effect (see Fig. 2). Its maximum tends progressively to the position of  $\text{Kr}_2^+\text{F}^-$  ( $4^2T \rightarrow 1^2T$ ) emission in solids, 453 nm, according to [6]. Thus, we conclude that this emission comes from triatomic excimers  $\text{Kr}_2^+\text{F}^-$  trapped in the cluster. After an excitation with a 10 eV photon the formation of a relaxed excimer  $\text{Kr}_2^+\text{F}^-$  releases

$\sim 2.4$  eV. Originally this energy is deposited into the reaction coordinate. It cannot be accumulated by small clusters, which obey a relatively low number of degrees of freedom. This apparently leads to an evaporation of krypton atoms (energy redistribution) or to an ejection of  $\text{Kr}^+\text{F}^-$  excimers from clusters (recoil mechanism). In contrast, because of a great difference in  $\text{Kr}^+\text{F}^-$  and  $\text{Kr}^+\text{Kr}$  potentials, ejection of  $\text{Kr}_2^+\text{F}^-$  excimers from the clusters is of low probability. Actually, we have not observed any fluorescence centered at 420 nm, characteristic of free  $\text{Kr}_2^+\text{F}^-$ . On the other hand, the released energy can be accommodated by larger clusters, which leads to an efficient stabilization and solvation of  $\text{Kr}_2^+\text{F}^-$  in clusters. For all these reasons the characteristic  $\text{Kr}^+\text{F}^-$  ( $\text{B} \rightarrow \text{X}$ ) emission at 5 eV disappears in large clusters. Because of the relatively large size distribution of clusters prepared by nozzle expansion ( $\Delta N \approx \bar{N}$ ), the experimental points in Figure 2 may not be true positioned along the  $\bar{N}$  axis. Because of this uncertainty about the true size the emission comes from, we could only qualitatively treat these results. We like to note that, although in ionized rare-gas clusters the positive charge may be localized on trimers [15,16], we have not assumed the formation of ionic  $(\text{Kr}_3^+\text{F}^-)^*$  compound. Indeed the DIM calculations [17] of another similar system,  $\text{Xe}_n^+\text{Cl}^-$ , have shown that the positive charge is localized on the dimer  $\text{Xe}_2^+$ .

For the interpretation of the new bands C and D it appears to be helpful to estimate the mean number of  $\text{NF}_3$  molecules  $\langle m \rangle$  deposited on the cluster. As generally, we have used a Poisson statistics to find the doping probability  $P_q(\langle m \rangle)$  of  $\text{Kr}_N$  clusters with  $q$  molecules [18,19]:

$$P_q(\langle m \rangle) = \frac{\langle m \rangle^q}{q!} \exp(-\langle m \rangle). \quad (1)$$

We assume that specific chemical reactions occurring in  $\text{Kr}_N(\text{NF}_3)_q$  clusters display the same  $P_q(\langle m \rangle)$  statistics. To relate the measured value of  $\text{NF}_3$  stagnation pressure ( $p_{\text{NF}_3}$ ) with  $\langle m \rangle$  in the above equation, we assume that formation of  $\text{Kr}_2^+\text{F}^-$ , which is responsible for the emission band B ( $I_B$ ) should evolve following a  $P_1$  law, when the  $\text{NF}_3$  pressure, and therefore  $\langle m \rangle$ , increases. Assuming that  $\langle m \rangle \propto p_{\text{NF}_3}$  we have fitted a curve  $P_1(p_{\text{NF}_3})$  through the experimental points of  $I_B$  in Figure 4. This calibration has been used to analyze the emission bands C and D.

Actually, using the above-discussed calibration, it has been found that the intensity of the emission band C follows a  $P_1(\langle m \rangle)$  law (see Fig. 4). Therefore, we attribute this emission to krypton clusters containing only one  $\text{NF}_3$  molecule:  $\langle m \rangle = 1$ . On the other hand, the emission D does not follow a pure  $P_2(\langle m \rangle)$  law but rather a sum of  $\sum_{i \geq 2} P_i$  one. This indicates that a deposition of at least two  $\text{NF}_3$  molecules on the cluster is needed for its observation. Finally, from the fluorescence intensity dependences of B, C and D bands we draw the conclusion that they result from different cluster composition. Bands B and C can be related to the same  $\text{Kr}_N\text{NF}_3$  clusters, while the band D has been attributed to the  $\text{Kr}_N(\text{NF}_3)_2$  clusters. Moreover, the

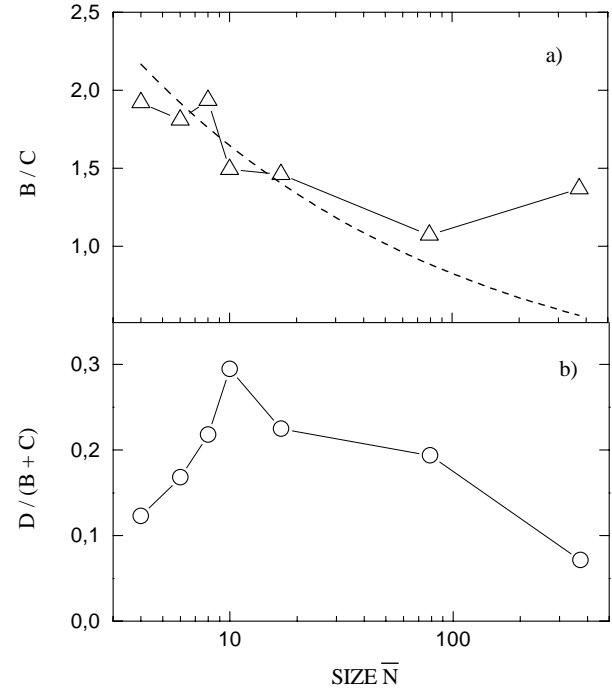


**Fig. 5.** Intensity ratio  $B/C$  and  $D/(B+C)$  as a function of the cluster size  $\bar{N}$  for a fixed stagnation pressure of  $\text{NF}_3$  (10 mbar). The dashed line in (a) shows an  $N^{-1/3}$  dependence.

emission band E growing at the highest  $\text{NF}_3$  cross-beam flow seems to require more than two  $\text{NF}_3$  molecules in the  $\text{Kr}_N$  cluster.

Now we give assignments for the remaining band C, D and E.

We assign the band C to the excimer  $\text{Kr}_2^+\text{NF}_3^-$  stabilized in the cluster. In the gas phase the electron attachment to  $\text{NF}_3$  leads to its fragmentation on  $\text{F}^- + \text{NF}_2$  with an excess kinetic energy of  $\sim 0.9$  eV [20]. In contrast to the gas phase, where the  $\text{NF}_3^-$  anion has never been observed, its formation in clusters may be possible due to a stabilization by the cluster environment, which actually has been recently observed in  $\text{Ar}_N\text{NF}_3^-$  clusters [21]. We believe that electron transfer results in the formation of a stable  $\text{Kr}_2^+\text{NF}_3^-$  excimer-like complex in  $\text{Kr}_N$  clusters. The red shift of the emission band C with respect to the  $\text{Kr}_2^+\text{F}^-$  emission (the band B) by  $0.18 \pm 0.02$  eV can be due, partly, to an extra charge-dipole interaction in the excimer involving  $\text{NF}_3^-$ , which is not the case of  $\text{F}^-$ .

The  $\text{NF}_3$  molecule seems to be not fixed on the surface and can migrate inside the cluster. Its likely position can be estimated by comparing the pair  $\text{Kr}-\text{NF}_3$  and  $\text{Kr}-\text{Kr}$  interactions and bond length, as has been previously discussed [22]. To our knowledge there are no data about  $\text{Kr}-\text{NF}_3$  potential available at present. Nevertheless, the  $\text{NF}_3$  molecule has a polarizability and size comparable with that of the  $\text{Kr}$  atom, and a small dipole moment. Therefore, we assume that there is no big differences between the  $\text{Kr}-\text{NF}_3$  and  $\text{Kr}-\text{Kr}$  interactions. Thus, we assume that the  $\text{NF}_3$  molecule can be solvated at the surface as well as in the interior of the cluster. This assumption is con-

firmed by the similarities observed in spectra obtained by the pick-up or coexpansion ( $[\text{Kr}]/[\text{NF}_3] = 1000/1$ ) techniques [23]. These results suggest an important mobility of the  $\text{NF}_3$  molecule in the krypton cluster.

The intensity ratio between bands B and C has been plotted in Figure 5a. It is generally accepted that the reaction dynamics can change with the cluster size from reactive to nonreactive one [24]. In the present case the localization of the  $\text{NF}_3$  molecule inside the cluster may prevent dissociation of the  $\text{NF}_3^-$  anion (cage effect) and favor the creation of a  $\text{Kr}_N\text{NF}_3$  excimer. One may suppose that the  $B/C$  intensity ratio will follow an  $N^{-1/3}$  dependence, which reflects the ratio between the surface and the bulk of the cluster. In fact, many factors like change in the  $\text{NF}_3$  mobility when the cluster grows, doping probability and orientation of  $\text{NF}_3$  inside the cluster, have to be considered, which makes a numerical treatment of the  $B/C$  intensity ratio difficult.

Band D is assigned to  $\text{Kr}_2^+(\text{NF}_3)_2^-$  in view of the pressure dependence (Fig. 4). When the  $\text{NF}_3$  pressure increases, the probability that two  $\text{NF}_3$  are picked up by the krypton cluster increases leading to the dimerization inside the cluster. Such process of dimerization has already been observed in argon clusters [25,26]. In a similar way, band E is attributed to complexes with at least three  $\text{NF}_3$ , namely  $\text{Kr}_2^+(\text{NF}_3)_3^-$ . The evolution of the intensity ratio  $D/(B+C)$  as a function of the size  $\bar{N}$  is shown in Figure 5b. In small clusters this ratio increases with  $\bar{N}$  since the cluster cross-section and doping probability increase. In large clusters ( $\bar{N} \geq 100$ ), because of the  $\text{NF}_3$  mobility discussed above, the probability for two  $\text{NF}_3$  molecules to find each other to form a dimer decreases with the cluster volume. This may explain the decrease of the  $D/(B+C)$  ratio in large clusters.

The red shift of the emission D with respect to C by  $\Delta E_{D-C} \simeq 0.18 \pm 0.02$  eV may be principally due to an additional stabilization of the anionic dimer  $(\text{NF}_3-\text{NF}_3)^-$ . This energy could be estimated from  $E_d = \frac{e}{4\pi\epsilon_0} \left( \frac{\mu_{\text{NF}_3}}{r^2} + \frac{e\alpha_{\text{NF}_3}}{2r^4} \right)$ , where  $\mu_{\text{NF}_3} = 0.234$  D and  $\alpha_{\text{NF}_3} = 3.62 \text{ \AA}^3$  are the permanent dipole moment and the polarizability of  $\text{NF}_3$ . The two terms in the previous equation characterize the charge dipole and charge-induced dipole interactions. Taking a typical intermolecular  $\text{NF}_3-\text{NF}_3$  distance to be  $r \simeq 4 \text{ \AA}$ , we found  $E_d = 0.14$  eV which is in good agreement with the experimental observations. For the emission E, which is attributed to the complex  $\text{Kr}_2^+(\text{NF}_3)_3^-$ , the binding energy of  $(\text{NF}_3)_3^-$  with respect to  $\text{NF}_3^-$  could be estimated as roughly  $2E_b = 0.28$  eV, which is again in agreement with the observed red shift of this emission respectively to the band C:  $\Delta E_{E-C} \simeq 0.34 \pm 0.06$  eV.

Surprisingly, we have not observed any red shift for the emission C and D when the cluster size increases. This seems indicate that this fluorescence comes from clusters larger than the estimated mean size  $\bar{N}$  which are in the high mass tail of the size distribution. Effectively, the  $\text{Kr}_2^+\text{NF}_3^-$  and  $\text{Kr}_2^+(\text{NF}_3)_2^-$  molecules are necessarily inside the cluster, since the  $\text{NF}_3^-$  anion needs to be stabilized by the surrounding krypton atoms. Therefore, when they radiate, these molecules are already solvated by a shell

of krypton atoms. The shift induced by krypton atoms of higher shell numbers is then small and difficult to observe.

## 5 Conclusion

In conclusion, charge-transfer reactions in  $\text{NF}_3$ -doped krypton clusters are reported. The fluorescence of  $\text{Kr}^+\text{F}^-$  excimers desorbing from clusters as well as solvated fluorescence species are observed following photoexcitation at 10 eV. In addition, fluorescence attributed to  $\text{Kr}_2^+(\text{NF}_3)_m^-$  complexes ( $m = 1, 2, 3 \dots$ ) has been observed. As it has already been discussed in [12], the reaction dynamics in the clusters differs considerably from that in the gas phase and solid samples. In particular the reaction pathways in clusters are inherently sensitive to the local environment on the scale of  $\sim 1$  nm, which is proved by the observed effects as a function of cluster size and composition. This is characteristic of the cluster phase in the sense that such precise environmental control is not possible in bulk solids. Moreover, thanks to fast sample renewal in cluster beams photo-reactions can be studied without complications due to the presence of reaction products. Financial support from the BMFT under grant 05 5GUAY Tpl is kindly acknowledged.

## References

1. D.W. Setser, J. Ku, in: *Photophysics and Photochemistry above 6 eV*, edited by F. Lahmani (Elsevier, Amsterdam, 1985) p. 621.
2. J. Ku, D.W. Setser, *Appl. Phys. Lett.* **48**, 689 (1986).
3. Alekseev, D.W. Setser, *J. Phys. Chem.* **100**, 5766 (1996).
4. M.E. Fajardo, V.A. Apkarian, *J. Chem. Phys.* **85**, 5660 (1986).
5. M.E. Fajardo, V.A. Apkarian, *J. Chem. Phys.* **89**, 4102 (1988).
6. H. Kunttu, J. Feld, R. Alimi, A. Becker, V.A. Apkarian, *J. Chem. Phys.* **92**, 4856 (1990).
7. H. Kunttu, E. Sekreta, V.A. Apkarian, *J. Chem. Phys.* **94**, 7819 (1991).
8. H. Kunz, J.G. McCaffrey, M. Chergui, R. Schriever, Ö. Ünal, V. Stepanenko, N. Schwentner, *J. Chem. Phys.* **95**, 1466 (1991).
9. *Excimer lasers, Topics in applied physics*, Vol. 30, edited by Ch.K. Rhodes, 2<sup>nd</sup> ed. (Springer Berlin-Heidelberg, 1984).
10. C. Dedonder-Lardeux, M. Berdah, C. Jouvét, S. Martrenchard-Barra, J.M. Mestdagh, D. Solgadi, J.P. Visticot, *J. Chem. Phys.* **104**, 2740 (1996).
11. C. Dedonder-Lardeux, C. Jouvét, S. Martrenchard-Barra, F. Talbot, D. Solgadi, *Chem. Phys. Lett.* **250**, 293 (1996).
12. L. Moussavizadeh, K. von Haeften, L. Museur, A.V. Kanaev, M.C. Castex, R. von Pietrowski, T. Möller, *Chem. Phys. Lett.* **305**, 327 (1999).
13. R. Karnbach, M. Joppien, J. Stapelfeldt, J. Wörmer, T. Möller, *Rev. Sci. Instrum.* **64**, 2838 (1993).
14. Z.J. Jabbour, K.A. Blanks, K.E. Martus, K. Becker, *J. Chem. Phys.* **88**, 4252 (1988).
15. M. Amarouche, G. Durand, J.P. Malrieu, *J. Chem. Phys.* **88**, 1010 (1987).

16. H. Haberland, B. von Issendorff, T. Kolar, H. Kornmeier, C. Ludewigt, A. Risch, *Phys. Rev. Lett.* **67**, 3290 (1991).
17. I. Last, T.F. George, *J. Chem. Phys.* **87**, 1183 (1987).
18. C. Gée, M.A. Gaveau, J.M. Mestdagh, M. Osborne, O. Sublemontier, J.P. Visticot, *J. Phys. Chem.* **100**, 13421 (1996).
19. J.M. Mestdagh, M.A. Gaveau, C. Gée, O. Sublemontier, J.P. Visticot, *Int. Rev. Phys. Chem.* **16**, 215 (1997).
20. T.M. Miller, J.F. Friedman, A.E. Stevens Miller, J.F. Paulson, *Int. J. Mass. Spectr. Ion Processes* **149/150**, 111 (1995).
21. L. Lehmann, S. Matjejcik, E. Illenberger, Y. Bouteiller, V. Periquet, L. Museur, C. Desfrancois, J.P. Schermann, *J. Phys. Chem. A* **101**, 9942 (1997).
22. L. Perera, F.G. Amar, *J. Chem. Phys.* **93**, 4893 (1990).
23. L. Moussavizadeh, Diplomarbeit, Universität Hamburg (1996).
24. J. Jortner, *Z. Phys. D* **24**, 247 (1992).
25. D.J. Levandier, M. Mengel, R. Pursel, J. McCombie, G. Scoles, *Z. Phys. D* **10**, 337 (1989).
26. D.J. Levandier, S. Goyal, J. McCombie, B. Pate, G. Scoles, *J. Chem. Soc. Faraday Trans.* **89**, 6069 (1990).